

Variable-ambient scanning stage for a laser scanning confocal microscope

D. J. Sirbulu, J. P. Schmidt, M. D. Mason, M. A. Summers, and S. K. Buratto^{a)}

Department of Chemistry and Biochemistry, University of California, Santa Barbara, California 93106

(Received 25 April 2003; accepted 19 June 2003)

A variable-ambient scanning stage for a laser scanning confocal microscope was designed and tested. The stage allows for facile observation of both thin films and single molecule samples under inert conditions. High precision images have been acquired up to $174 \mu\text{m}^2$ using a single piezoceramic tube. The vacuum seal is achieved by simply placing the sample side of a standard 25×25 mm glass coverslip face down onto a Buna o ring and gently clamping it in place with a Teflon cap. Tests show that the stage holds a vacuum of at least 3×10^{-6} Torr. Fluorescence experiments performed on films of an organic dye, DiI_{C12}, as well as single molecule experiments performed on air sensitive oligo(phenylenevinylene) molecules, effectively demonstrate the ability of the scanner to reduce photo-oxidation rates. © 2003 American Institute of Physics.

[DOI: 10.1063/1.1599073]

I. INTRODUCTION

Advances in ultrasensitive optical detection and imaging have made the study of single molecules (SMs) possible. Single molecule spectroscopy has become immensely popular due to the wide variety of photophysical phenomena observed that are masked in ensemble measurements such as discrete intensity fluctuations,^{1–8} changes in spectral position and line shape,^{1,7,9} photon antibunching,^{10,11} and polarized excitation effects.^{1,3,12} These photophysical processes yield valuable information regarding both the fundamental nature of molecular emission and the effect of the nanoenvironment. These techniques are limited, however, by the relatively short time a single molecule emits photons due to photodegradation processes.

In well-studied systems such as the fluorescent dye “DiI” and other fluorescent probes, triplet–triplet interactions with oxygen increase the nonradiative T_1-S_0 probability.¹³ Singlet oxygen forms as a result of the triplet–triplet interactions and can lead to irreversible photo-oxidation. In addition, previous studies of DiI adsorbed on glass, or embedded in a polymer, show that triplet–triplet annihilation increases as the partial pressure of oxygen increases.^{13–16} Oxygen poisoning is especially problematic in the study and production of organic light emitting diodes (OLEDs) due to the destruction of conjugation caused by photogenerated singlet oxygen.

Most attempts to remove deleterious species such as oxygen in laser scanning confocal microscopy experiments have consisted of encapsulating the sample to inhibit oxygen diffusion. Thin polymer films of poly (methyl methacrylate) (PMMA), polyvinylbutyral (PVB),¹⁷ or other polymers,¹⁸ have been utilized as encapsulating layers,¹⁹ as well as thermally evaporated metal films which bind oxygen before it can diffuse into the sample.¹³ While these methods decrease the rate of photodegradation, they also alter the nanoscale environment. Polymer encapsulating layers physically inhibit

the conformational dynamics of the imbedded molecules, and metal can quench fluorescence if the molecules are placed in close proximity to it.

In order to maintain sample integrity and to minimize preparation time, we have focused our efforts on designing a scanning stage that allows virtually any thin film material to be placed in an oxygen-free environment without sample manipulation. We have successfully constructed a piezoceramic vacuum stage that performs equally well in comparison with ambient piezoceramic scanning stages. This stage allows the sample to be evacuated or purged with the desired inert gas for a multitude of potential applications. The scanning stage described herein was successfully integrated with our custom-built laser scanning confocal microscope (LSCM).⁸ The following sections provide details on the construction process of the scanner as well as experimental results validating its performance.

II. INSTRUMENTATION

Figure 1 shows a picture and schematic of the vacuum LSCM stage. A brass foundation was constructed to minimize stress on the piezotube, while at the same time providing a feasible means of repairing the stage without damaging the tube. The brass base consists of three components, two side supports that clamp the bottom of the piezotube, and a central support that holds the 90° hose adapter. The hose adapter is also secured by a small Allen bolt that is threaded through the side of the central support. The hose adapter connects the internal bellows tube to the quick release vacuum port (Swagelok) using a $\frac{1}{4}$ in. XOA adapter (Swagelok) to seal the connection. The bellows is welded to the bottom of the head piece. Once assembled, the bellows holds most of the head-piece weight. In addition, it provides the necessary $x-y$ mobility of the piezoceramic.

The piezotube has a parallel axis sectioned into 4°–90° quadrants (Stavely Sensors, Inc.). Each quadrant has soldered wires that run directly to the Digital Instruments scanning electronics. The piezotube length, outer diameter, and

^{a)}Electronic mail: buratto@chem.ucsb.edu

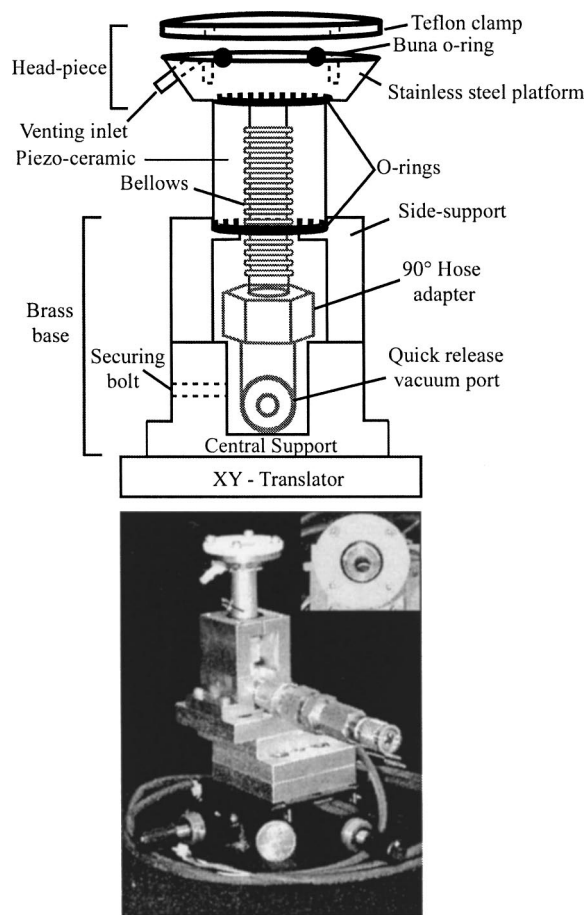


FIG. 1. Schematic drawing of the scanning stage (left) and digital picture with the inset of the head piece (right). The sample sits inverted clamped between the Buna o ring and Teflon top. Electrical contacts were soldered to the outside of the piezotube.

wall thickness are 2.54, 1.27, and 0.076 cm, respectively. Plastic rings are rigidly fixed to the piezotube to eliminate current shorts. The piezotube/plastic ring assembly is glued at the top to the head piece and clamped at the bottom by the two brass side supports.

The head piece consists of the stainless steel platform, Teflon clamp, and venting inlet. After spin casting the sample onto a microscope cover glass (0.19–0.25 mm thick), it is inverted, and placed on a slightly elevated Buna o ring inside the stainless steel head piece. The Teflon clamp is then finger tightened with bolts to compress the o ring and completely seal the inner chamber.

III. PERFORMANCE

Figure 2 shows a $10 \times 10 \mu\text{m}$ laser reflection scan of a silicon refraction grid patterned with $1.2 \mu\text{m}$ squares. The grid was used for calibrating the instrument and determining the scanning capabilities of the stage. After calibrating the scanner, a maximum scan size of $13.2 \times 13.2 \mu\text{m}$ was achieved. Even more importantly, the scanner displayed smooth scan lines over its entire range despite the added weight of the vacuum assembly. It was also apparent in the reflection images that the scanner head had a near 0° head tilt. The scanner was then tested for leaks, and whether the ~ 0.2 -mm-thick cover slips could hold the vacuum. The

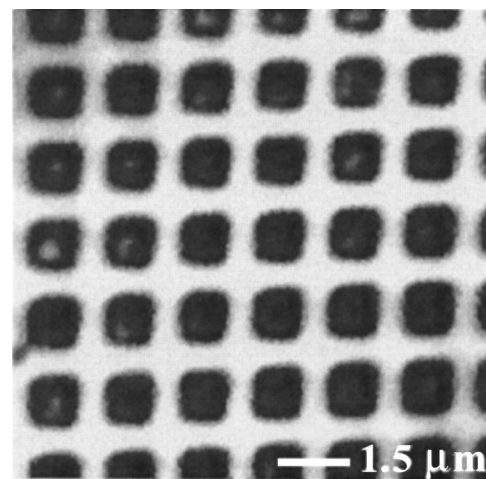


FIG. 2. Laser reflection scan of a silicon refracting grid patterned with $1.2 \mu\text{m}$ squares. The grid was used to calibrate and determine the limitations of the scanner. The maximum scanning range is $174 \mu\text{m}^2$.

scanner successfully held a vacuum of 3×10^{-6} Torr over 10 min. It is also possible to purge the chamber with an inert gas, such as nitrogen, to provide anaerobic conditions at ambient pressure.

A well-studied dye (DiIC_{12}) was chosen for the initial oxygen/vacuum experiments. A film was prepared by spin casting $25 \mu\text{L}$ of a $100 \mu\text{M}$ DiI chloroform solution on a microscope cover glass. After pumping on the sample for 10 min with a standard oil mechanical pump ($\sim 10^{-3}$ Torr), the film was illuminated using the 488 nm line of an argon-ion laser (Spectra Physics). The laser was focused to a near-diffraction-limited spot and positioned over a fresh area in the film. Spectra were taken at 6 s integration times while the excitation source remained fixed over the sample. The resulting spectra were fit to three Gaussians and integrated to obtain an arbitrary total intensity value. Figure 3 shows a plot of the normalized integrated intensity versus exposure time under vacuum [curve (a)] and in air [curve (b)]. The plots were fit to two exponentials giving fast decay time constants of 24 and 87 s for air and vacuum, respectively. The slow time constants for air and vacuum were 127 and 1491 s, respectively. The dramatic decrease in the photo-oxidation rate was achieved after only 10 min in vacuum. Samples are, typically, evacuated for several hours.

Using the vacuum scanner we also performed single

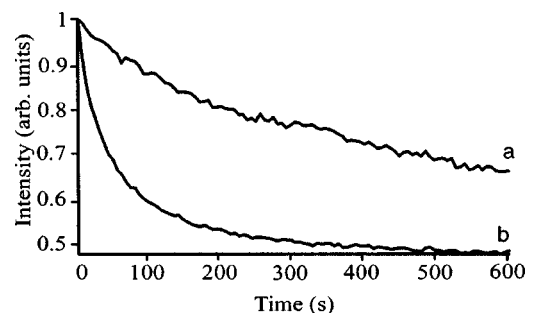


FIG. 3. Plot of the normalized integrated intensity versus exposure time for a film of DiIC_{12} in vacuum (a) and air (b). Sample was prepared by spin casting $25 \mu\text{L}$ of a $100 \mu\text{M}$ DiI solution.

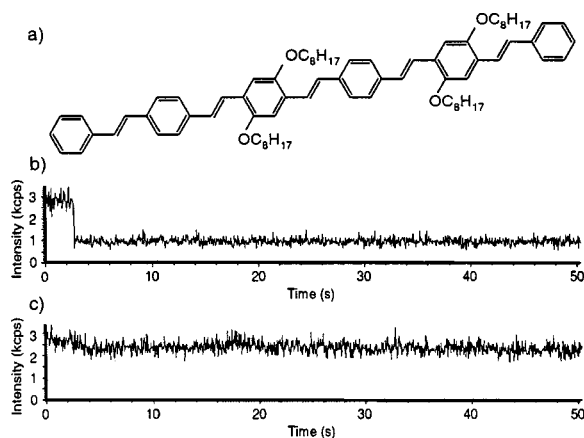


FIG. 4. (a) Structure of the soluble oligo(phenylenevinylene) molecule used in this study, denoted 6R-OC₈H₁₇. (b) Intensity trajectory for a single 6R-OC₈H₁₇ molecule in the presence of air. Data were collected using the scanner described in this article, but without the flow of N₂ through the sample chamber. (c) Intensity trajectory for a single 6R-OC₈H₁₇ molecule in a N₂ environment. Data were collected using the scanner described in this article under a positive pressure of N₂. The two intensity trajectories were collected using approximately the same laser intensity ($\lambda=457.9$ nm).

molecule spectroscopy on a series of highly air sensitive oligo(phenylenevinylene) (OPV) molecules (Fig. 4).^{20,21} In the presence of air, these molecules rapidly and irreversibly photobleach, as seen in the single molecule intensity trajectory in Fig. 4(b). Here, the molecule is fluorescing for only ~ 3 s and then photobleaches. Because of the short “on” times in air, it was nearly impossible to obtain data for these small molecules before the vacuum stage was built. We have found that maintaining a focused laser beam with the vacuum stage can be problematic due to the concave distortion of the cover glass under vacuum. However, it is possible to use a thicker cover glass or to backfill the chamber of the stage with high-purity nitrogen to maintain an oxygen- and water-free environment. For single molecule spectroscopy, the vacuum stage sample chamber is evacuated with a mechanical pump for approximately 1 h. A positive pressure of nitrogen is then introduced into the chamber, and a low flow rate is maintained throughout the experiments. Before entering the sample chamber the nitrogen passes through anhydrous calcium sulfate pellets and an oxygen scrubber (Altech OxyPurge-N) to remove residual water and oxygen, respectively. The intensity trajectory in Fig. 4(c) shows data collected for a single oligo(phenylenevinylene) molecule in a

nitrogen environment. We have observed continuous emission from single OPV molecules for over 10 min under these conditions.

In conclusion, we have constructed a variable ambient scanning stage for a laser confocal microscope. The stage setup eliminates unnecessary sample preparation to remove oxygen during experimentation. In addition, the stage’s configuration allows oil immersion objectives to be used, increasing the signal to noise. Future additions to the stage include a refrigeration system integrated with a thermocouple, and ideas to increase the scanning size are also being explored.

- ¹X. S. Xie and R. C. Dunn, *Science* **265**, 361 (1994).
- ²W. P. Ambrose, P. M. Goodwin, J. C. Martin, and R. A. Keller, *Phys. Rev. Lett.* **72**, 160 (1994).
- ³T. Ha, T. Enderle, D. S. Chemla, P. R. Selvin, and S. Weiss, *Phys. Rev. Lett.* **77**, 3979 (1996).
- ⁴T. Ha, T. Enderle, D. S. Chemla, P. R. Selvin, and S. Weiss, *Chem. Phys. Lett.* **271**, 1 (1997).
- ⁵R. M. Dickson, A. B. Cubitt, R. Y. Tsien, and W. E. Moerner, *Nature (London)* **388**, 355 (1997).
- ⁶D. A. VandenBout, W. T. Yip, D. H. Hu, D. K. Fu, T. M. Swager, and P. F. Barbara, *Science* **277**, 1074 (1997).
- ⁷K. D. Weston, P. J. Carson, H. Metiu, and S. K. Buratto, *J. Chem. Phys.* **109**, 7474 (1998).
- ⁸K. D. Weston and S. K. Buratto, *J. Phys. Chem. A* **102**, 3635 (1998).
- ⁹J. J. Macklin, J. K. Trautman, T. D. Harris, and L. E. Brus, *Science* **272**, 255 (1996).
- ¹⁰C. W. Hollars, S. M. Lane, and T. Huser, *Chem. Phys. Lett.* **370**, 393 (2003).
- ¹¹P. Michler, A. Imamoglu, M. D. Mason, P. J. Carson, G. F. Strouse, and S. K. Buratto, *Nature (London)* **406**, 968 (2000).
- ¹²F. Güttler, J. Sepiol, T. Plakhotnik, A. Mitterdorfer, A. Renn, and U. P. Wild, *J. Lumin.* **56**, 29 (1993).
- ¹³D. S. English, A. Furube, and P. F. Barbara, *Chem. Phys. Lett.* **324**, 15 (2000).
- ¹⁴K. D. Weston, P. J. Carson, and S. K. Buratto, *Chem. Phys. Lett.* **308**, 58 (1999).
- ¹⁵W.-T. Yip, D. Hu, J. Yu, D. A. V. Bout, and P. F. Barbara, *J. Phys. Chem. A* **102**, 7564 (1998).
- ¹⁶J. A. Veerman, M. F. Garcia-Parajo, L. Kuipers, and N. F. van Hulst, *Phys. Rev. Lett.* **83**, 2155 (1999).
- ¹⁷T. Huser, M. Yan, and L. J. Rothberg, *P. Natl. Acad. Sci. USA* **97**, 11187 (2000).
- ¹⁸J. Yu, H. Dehong, and P. F. Barbara, *Science* **289**, (2000).
- ¹⁹J. D. White, J. H. Hsu, W. S. Fann, S.-C. Yang, G. Y. Pern, and S. A. Chen, *Chem. Phys. Lett.* **338**, 263 (2001).
- ²⁰M. A. Summers, P. R. Kemper, J. E. Bushnell, M. R. Robinson, G. C. Bazan, M. T. Bowers, and S. K. Buratto, *J. Am. Chem. Soc.* **125**, 5199 (2003).
- ²¹M. R. Robinson, S. Wang, A. J. Heeger, and G. C. Bazan, *Adv. Funct. Mater.* **11**, 413 (2001).